Expanded View Figures

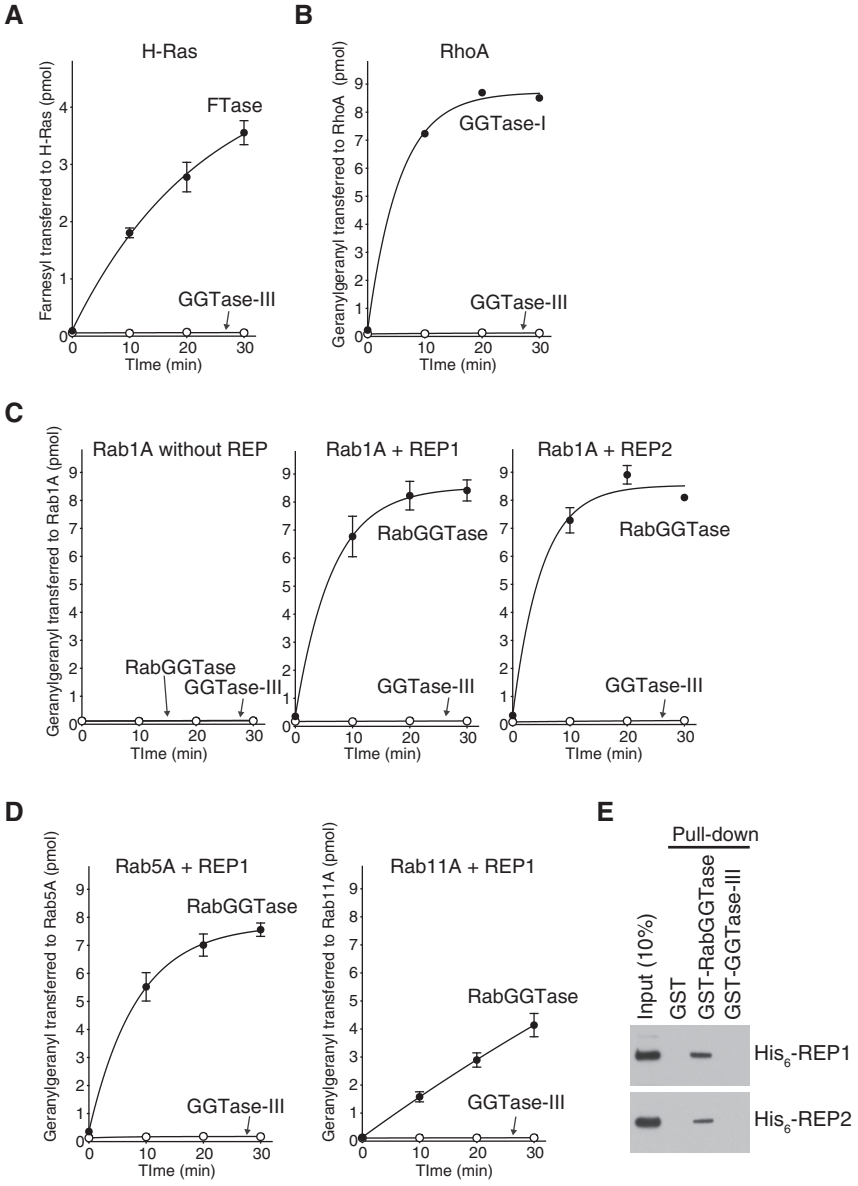

Figure EV1. GGTase-III has no prenyltransferase activity on known prenyltransferase substrates.

A–D Prenylation activity of GGTase-III on Ras, Rho, and Rab proteins. (A) His_6-H-Ras (5 μM) was incubated with FTase (50 nM) or GGTase-III (50 nM) and ^{3}H-FPP (1 μM) at 37°C. Reactions were stopped at the indicated time points, and the amount of ^{3}H-farnesyl transferred to H-Ras was quantified by scintillation counting (mean ± SEM, n = 3). (B) His_6-RhoA (5 μM) was incubated with GGTase-I (50 nM) or GGTase-III (50 nM) and ^{3}H-GGPP (1 μM), and the amount of ^{3}H-geranylgeranyl transferred to RhoA was quantified (mean ± SEM, n = 3). (C) His_6-Rab1A (5 μM) was incubated with RabGGTase (50 nM) or GGTase-III (50 nM) and ^{3}H-GGPP (1 μM) in the absence or presence of either His_6-REP1 (100 nM) or His_6-REP2 (100 nM), and the amount of ^{3}H-geranylgeranyl transferred to Rab1A was quantified (mean ± SEM, n = 3). (D) His_6-Rab5A and His_6-Rab11A were incubated with RabGGTase (50 nM) or GGTase-III (50 nM) and ^{3}H-GGPP (1 μM) in the presence of His_6-REP1 (100 nM), and the amount of ^{3}H-geranylgeranyl transferred to Rab5A and Rab11A was quantified (mean ± SEM, n = 3).

E REP pull-down assay. Recombinant His_6-REP1 or His_6-REP2 was incubated with glutathione Sepharose beads coated with GST, GST-RabGGTase, or GST-GGTase-III. Bound His_6-REP proteins were analyzed by immunoblotting with anti-His_6 antibody.

Source data are available online for this figure.

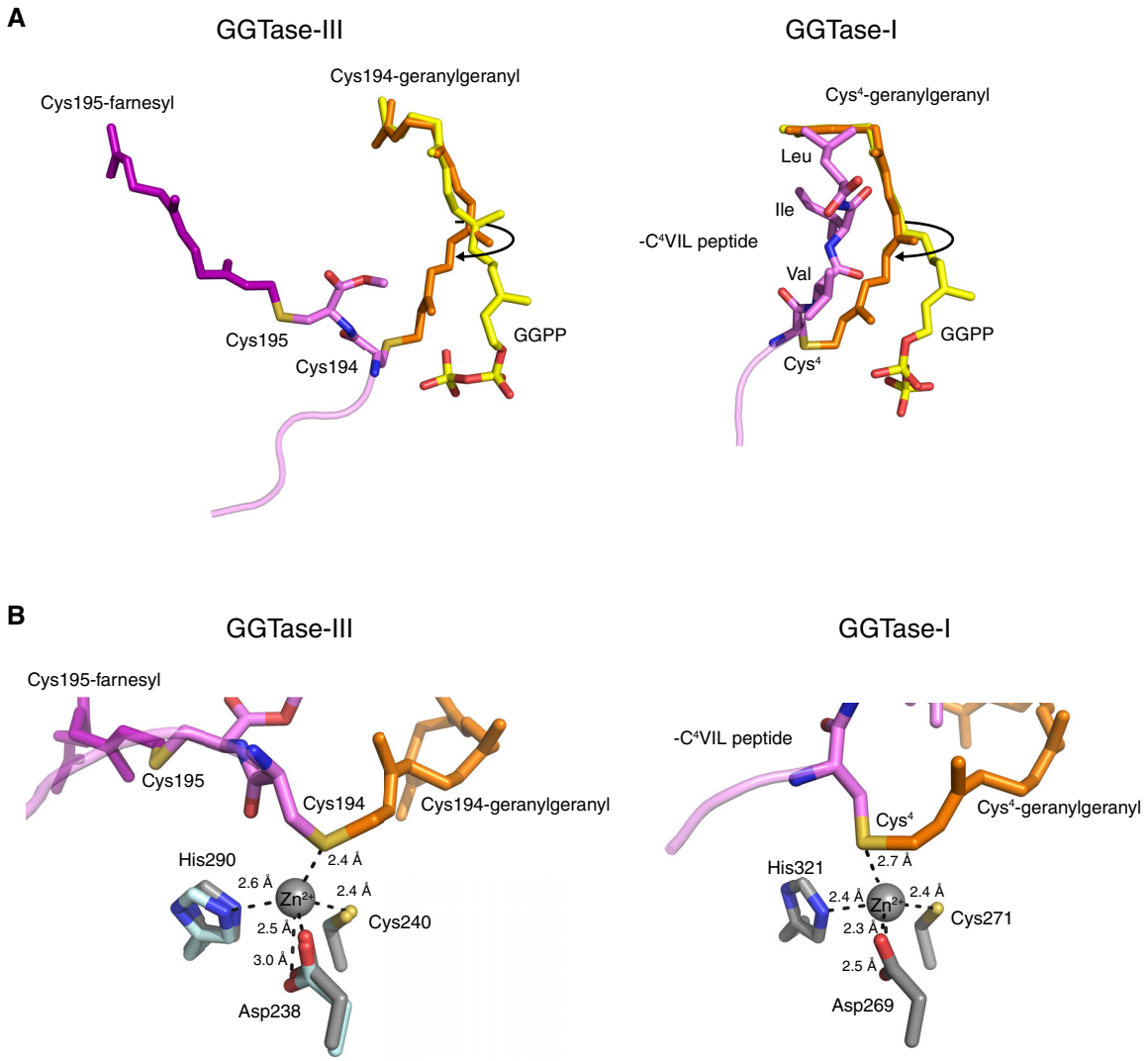

Figure EV2. Active site of GGTase-III.

A Left, comparison of the Cys194-linked geranylgeranyl moiety (orange) in the GGTase-III–product complex and GGPP (yellow) in the GGTase-III–GGPP complex. In the product complex, the first and second isoprene units of GGPP are rotated to form a covalent bond with Cys194. The Cys195-linked farnesyl moiety (purple) is anchored into the hydrophobic tunnel. Right, comparison of the geranylgeranyl moiety (orange) linked to Cys^4 of C^4VIL peptide in the GGTase-I–product complex (PDB 1N4R) and GGPP (yellow) in the GGTase-I–GGPP complex (PDB 1N4P). GGTase-III and GGTase-I show similar isoprene movements during catalysis.

B Left, the catalytic zinc ion and zinc-coordinating residues of RabGGTase (gray; PDB 3DST) superposed on the GGTase-III–product complex (cyan). The sulfur atom of geranylgeranylated Cys194 is located in the vicinity of the superposed catalytic zinc ion. Right, the catalytic site of the GGTase-I–product complex (PDB 1N4R). GGTase-III has a similar active site arrangement as GGTase-I.

Figure EV3. Generation of PTAR1 KO cells by CRISPR-Cas9 genome editing.

A Generation of PTAR1 KO cell lines by CRISPR-Cas9 using single-guide RNA (sgRNA) targeting exon 2 of the human PTAR1 gene. The target sequence and PAM sequence are indicated.

B Sequence data of the genomic region containing the exon 2 of PTAR1. Insertion and deletion mutations are shown in red, and the resulting premature stop codons are underlined. These mutations introduce a stop codon at the amino acid position 42 or 43. HAP1 is a haploid cell line and contains a single allele for PTAR1. nt, nucleotide.

C Immunoblot analysis of WT cells, PTAR1 KO cells, and PTAR1 KO cells stably expressing PTAR1 (KO + PTAR1) using anti-PTAR1 antibody. Asterisks denote proteins that cross-react with the antibody.

D Cytosolic localization of Ykt6 in HeLa cells. WT and PTAR1 KO HeLa cells were fractionated into cytosol and membrane fractions, and analyzed by immunoblotting with anti-syntaxin 5 and anti-Ykt6 antibody. Syntaxin 5 has two isoforms with different translation initiation sites.

E Prenylation status of Ykt6 in PTAR1 KO HAP1 cells and PTAR1 KO HAP1 cells stably expressing WT PTAR1 or Yk6-binding defective mutants of PTAR1. The prenylation status of Ykt6 was analyzed by DOC-PAGE followed by immunoblotting with anti-Ykt6 antibody. Lower panels show conventional immunoblot analysis of the same samples using the indicated antibodies.

Source data are available online for this figure.

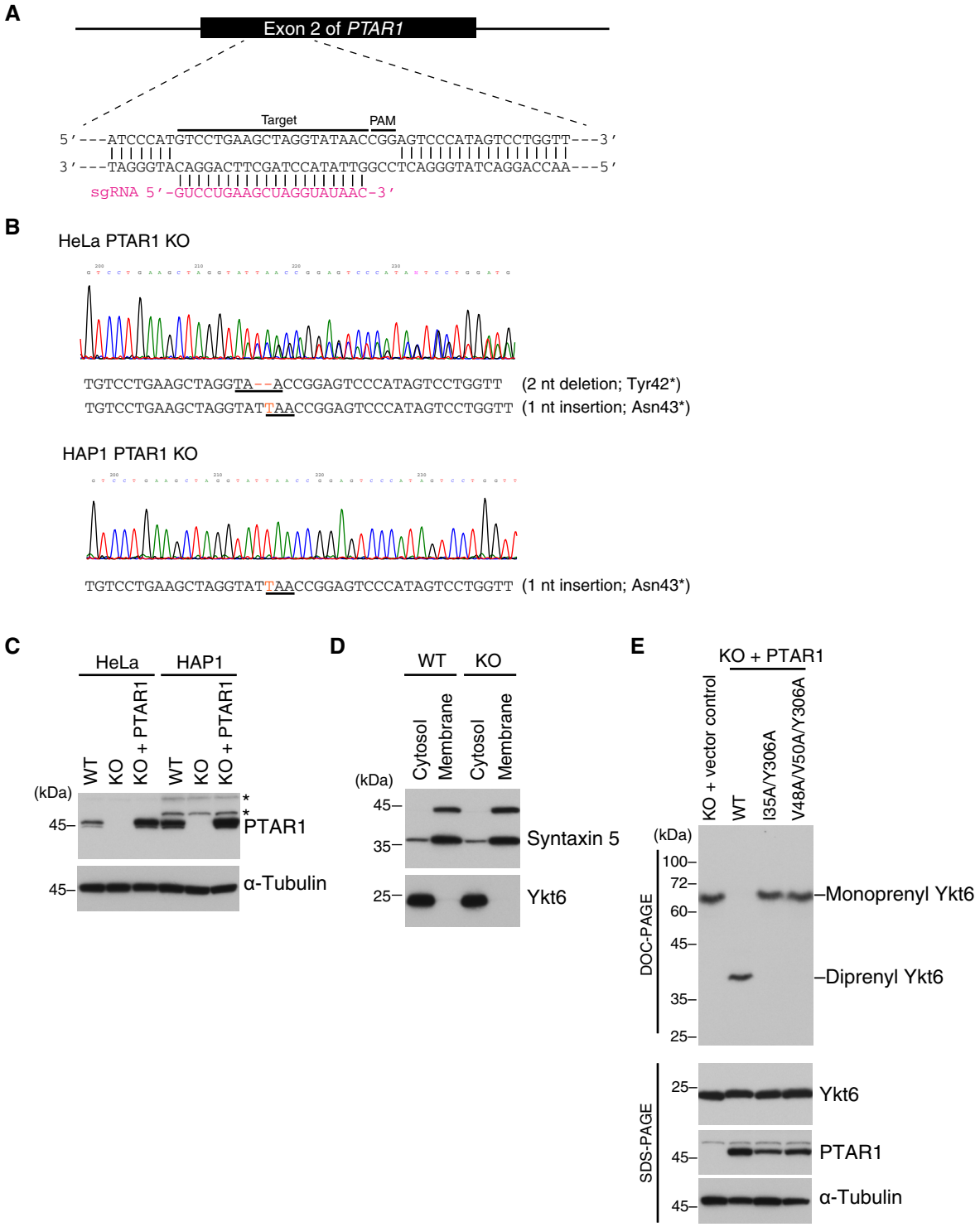

Figure EV3.

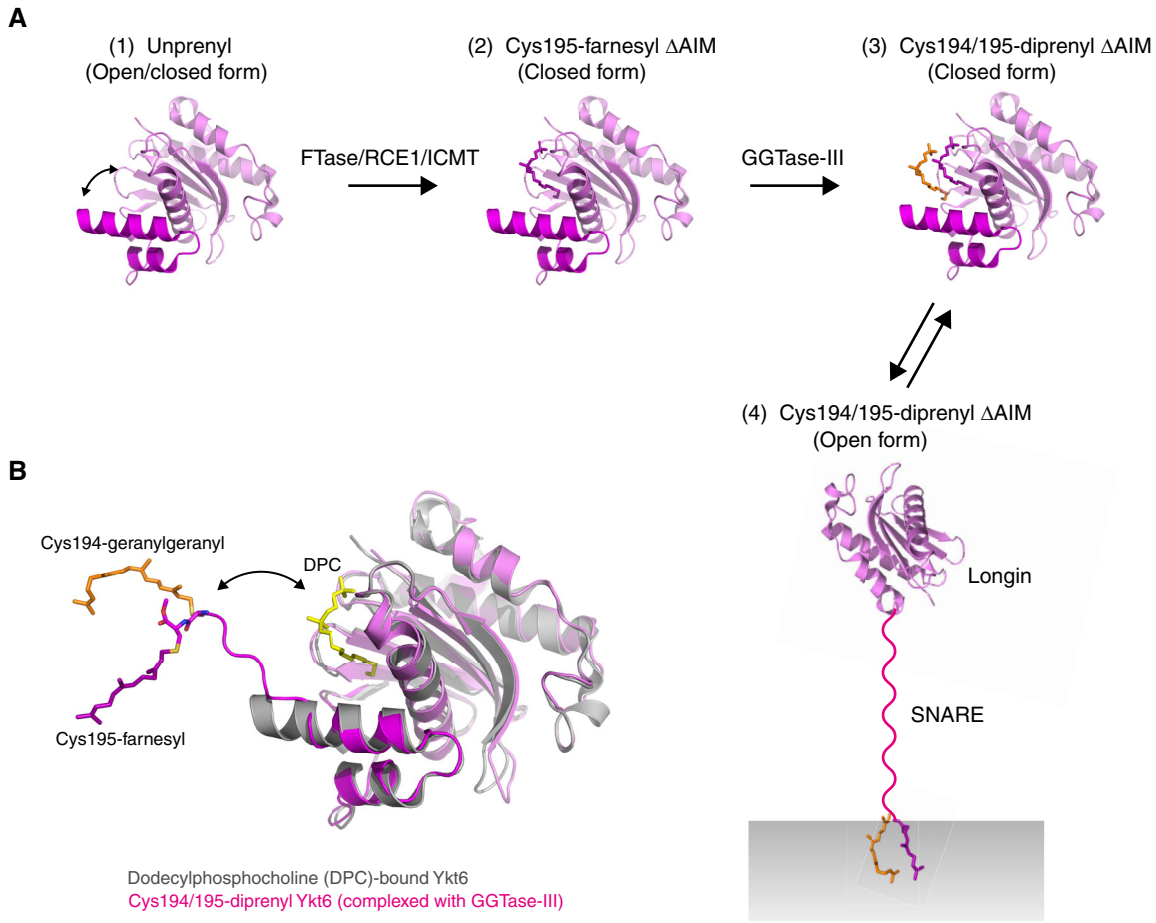

Figure EV4. Scheme of the double prenylation of Ykt6.

A Model for the sequential double prenylation of Ykt6. (1) Nascent unprenylated Ykt6 exists in both closed and open conformations. (2) Farnesylation of Cys195 stabilizes the closed conformation of Ykt6. (3) Doubly prenylated Ykt6 keeps the closed conformation by sequestering both farnesyl and geranylgeranyl groups into the putative prenyl binding groove. (4) Upon activation, the SNARE domain is unfolded and the C-terminal two prenyl groups are inserted into the membrane.

B Superposition of the dodecylphosphocholine (DPC)-bound, closed form of Ykt6 (gray; PDB 3KYQ) and Cys194/195-diprenyl Ykt6$^{\Delta AIM}$ complexed to GGTase-III (longin, pink; SNARE, magenta). GGTase-III is omitted for clarity. The putative prenyl binding groove of Ykt6, occupied by DPC (yellow), is located closed to the active site of the enzyme. Upon binding to GGTase-III, the Cys195-linked farnesyl moiety accommodated in the putative prenyl binding groove of Ykt6 is translocated into the hydrophobic tunnel of the enzyme, allowing the transfer of geranylgeranyl moiety to Cys194. The attached two prenyl groups may easily translocate back to the prenyl binding groove of Ykt6.

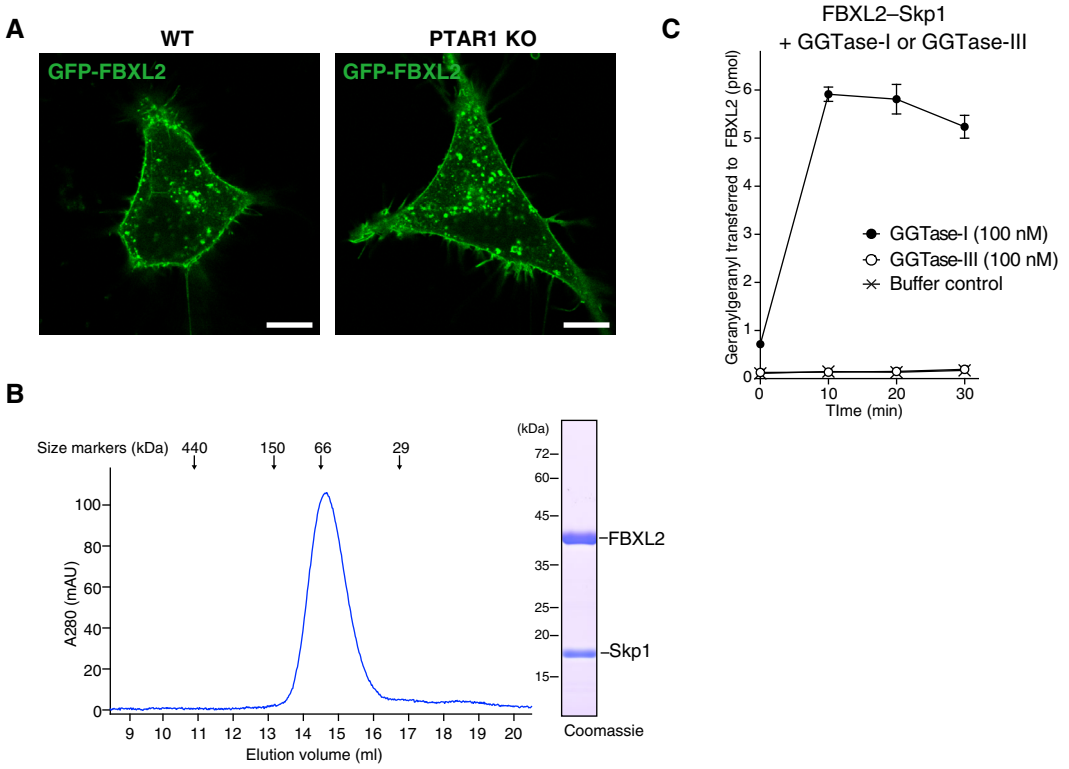

Figure EV5. GGTase-III cannot geranylgeranylate FBXL2.

A Localization of FBXL2 in HeLa cells. WT HeLa cells and PTAR1 KO HeLa cells transiently expressing GFP-FBXL2 and myc-Skp1 were observed for GFP fluorescence. In PTAR1 KO cells, GFP-FBXL2 was still able to localize to the plasma membrane as observed in WT cells. Scale bars, 10 μm.

B Purification of the recombinant FBXL2–Skp1 complex by Superdex 200 gel filtration chromatography. The peak fraction was analyzed by SDS–PAGE and Coomassie staining.

C Geranylgeranylation assay showing that GGTase-III cannot geranylgeranylate FBXL2. The purified recombinant FBXL2–Skp1 complex (5 μM) was incubated with GGTase-I (100 nM) or GGTase-III (100 nM) and ^{3}H-GGPP (1 μM) at 37°C. Reactions were stopped at the indicated time points, and the amount of ^{3}H-geranylgeranyl transferred to FBXL2 was quantified by scintillation counting (mean ± SEM, n = 3). GGTase-III failed to geranylgeranylate FBXL2, whereas GGTase-I efficiently geranylgeranylated FBXL2 under the same conditions.

Source data are available online for this figure.